

Lower critical dimension of the random-field XY model and the zero-temperature critical line

Kutay Akin^{1,2} and A. Nihat Berker^{3,4,5}

¹*Department of Electrical and Electronics Engineering, Boğaziçi University, Bebek, Istanbul 34342, Turkey*

²*Department of Physics, Boğaziçi University, Bebek, Istanbul 34342, Turkey*

³*Faculty of Engineering and Natural Sciences, Kadir Has University, Cibali, Istanbul 34083, Turkey*

⁴*TÜBITAK Research Institute for Fundamental Sciences, Gebze, Kocaeli 41470, Turkey*

⁵*Department of Physics, Massachusetts Institute of Technology, Cambridge, Massachusetts 02139, USA*



(Received 17 May 2022; accepted 5 July 2022; published 29 July 2022)

The random-field XY model is studied in spatial dimensions $d = 3$ and 4, and in between, as the limit $q \rightarrow \infty$ of the q -state clock models, by the exact renormalization-group solution of the hierarchical lattice or, equivalently, the Migdal-Kadanoff approximation to the hypercubic lattices. The lower critical dimension is determined between $3.81 < d_c < 4$. When the random field is scaled with q , a line segment of zero-temperature criticality is found in $d = 3$. When the random field is scaled with q^2 , a universal phase diagram is found at intermediate temperatures in $d = 3$.

DOI: [10.1103/PhysRevE.106.014151](https://doi.org/10.1103/PhysRevE.106.014151)

I. INTRODUCTION: ISING AND XY LOWER CRITICAL DIMENSIONS

Quenched randomness strongly affects the occurrence of order at low spatial dimension d , reflected as the lower-critical dimension d_c below which no ordering occurs for a given class of systems. In the random-magnetic-field $n = 1$ component spin Ising model, after a strong experimental and theoretical controversy between $d_c = 2$ claims [1–3] and $d_c = 3$ claims [4], the issue was settled for $d_c = 2$ [5,6]. The fact that d_c is not 3 fell in contradiction with the prediction of a dimensional shift of two due to random fields coming from all-order field-theoretic expansions from $d = 6$ down to $d = 1$ [7], which indeed is a considerable distance to expand upon for a small-parameter expansion of $\epsilon = 6 - d$. In this study, the logically next model, namely the $n = 2$ components spin-XY model under random fields is examined and surprising results are obtained, this time in near agreement with the dimensional shift of two, but also with an interesting zero-temperature critical line segment and a universal scaled finite-temperature phase diagram.

Random-field Ising results supporting $d_c = 2$ were obtained [5,6] by the Migdal-Kadanoff [8,9] renormalization-group calculations in $d = 2$ (no random-field order), $d = 2.32$ (random-field order), and $d = 3$ (more random-field order). In the same vein, for the random-field XY model, Migdal-Kadanoff renormalization-group calculations are done here in $d = 3$ and 4, and in between. The Migdal-Kadanoff renormalization-group calculation (Fig. 1) is a highly successful, flexible, and therefore most used to date and today, physically motivated approximation for hypercubic lattices and, simultaneously, an exact calculation for d -dimensional hierarchical lattices [10–12]. The hierarchical lattice connection makes the Migdal-Kadanoff procedure a physically realizable approximation. For recent work using hierarchical lattices, see Refs. [13–24]. Migdal-Kadanoff-hierarchical lattices correctly give the lower critical dimensions of $d_c =$

1 of the Ising model [8,9], $d_c = 2$ of the XY [25,26], and ($n = 3$ spin components) Heisenberg [27] models in the absence of quenched randomness. For the much more complex system with competing quenched-random interactions, Migdal-Kadanoff gives the noninteger $d_c = 2.46$ for the Ising spin-glass system [28–34]. In addition to giving the lower critical dimensions, it yields such diverse results as, e.g., the low-temperature algebraic order of the $d = 2$ XY model [25,26], the chaotic nature [35–37] of the ferromagnetic-antiferromagnetic [38] and left-right chiral [39] Ising spin glasses, and the changeover from second- to first-order phase transitions of q -state Potts models in $d = 2$ and 3 [40].

II. MODEL AND METHOD

The XY model is approached as the $q \rightarrow \infty$ limit of the q -state clock models. For other works on the random-field XY model, see Refs. [41–45]. In the q -state clock models, at each site i of the lattice, a planar unit spin \vec{s}_i can point in one of q directions in the plane, namely with the angle $\theta_k = k(2\pi/q)$, where $k = 0, 1, \dots, q - 1$. A detailed renormalization-group study on the phase transitions and thermodynamics of the q -state clock models, without quenched randomness, has been done [24]. The currently studied q -state clock model, with quenched random fields, is defined by the Hamiltonian

$$-\beta\mathcal{H} = \sum_{\langle ij \rangle} (J\vec{s}_i \cdot \vec{s}_j + \vec{s}_i \cdot \vec{H}_i + \vec{s}_j \cdot \vec{H}_j), \quad (1)$$

where $\beta = 1/k_B T$ and sum is over all nearest-neighbor pairs of spins. In each term in the sum, the random fields \vec{H}_i, \vec{H}_j have magnitude H and each randomly points along one of the allowed directions θ_k .

We solve this model using the Migdal-Kadanoff renormalization group. The local renormalization-group transformation is given in Fig. 1 and is simple to implement in

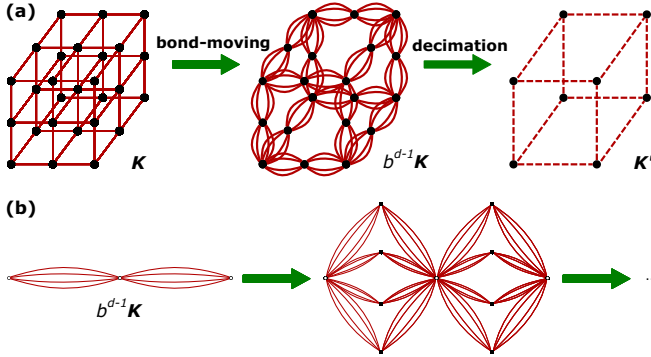


FIG. 1. From Ref. [24]: (a) Migdal-Kadanoff approximate renormalization-group transformation for the $d = 3$ cubic lattice with the length-rescaling factor of $b = 2$. (b) Construction of the $d = 3$, $b = 2$ hierarchical lattice for which the Migdal-Kadanoff recursion relation is exact. For general spatial dimension d , the bond moving is (b^{d-1}) -fold. The renormalization-group solution of a hierarchical lattice proceeds in the opposite direction of its construction.

systems without quenched randomness. In both steps of the transformation, the magnetic field terms of the input bonds are added with their own direction and magnitude, which reflects their microscopic effect on the system. After the first transformation, there is a distribution of random-field magnitudes and directions (extending the original clock directions of the unrenormalized system). With our currently studied quenched random-field model, the renormalization-group evolution of quenched random distributions has to be pursued. Initially, 5000 nearest-neighbor Hamiltonians are created, with 10000 randomly chosen magnetic field directions as described above. From this distribution, b^d nearest-neighbor Hamiltonians are randomly chosen, to effect the local Migdal-Kadanoff transformation and obtain a

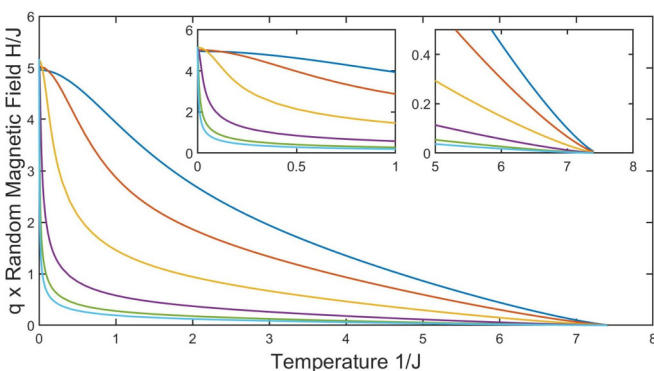


FIG. 2. Phase diagrams for $(q = 7, 10, 20, 50, 100, 150)$ -state random-field clock models in $d = 3$, occurring in the figure, respectively, from high field to low field. Disordered and ferromagnetic phases occur at high temperature-high field and low temperature-low field, respectively. It is seen that the ferromagnetic phase, in random field, disappears as $q \rightarrow \infty$, indicating that no ferromagnetic phase occurs in the random-field XY model at nonzero temperature in $d = 3$. However, for high q , the ordered phase extends to $qH/J = 5.1$ at zero temperature, as also seen in the left inset. For high q , the zero-field ferromagnetic transition temperature saturates, as also seen in Ref. [24] and in the right inset in this figure.

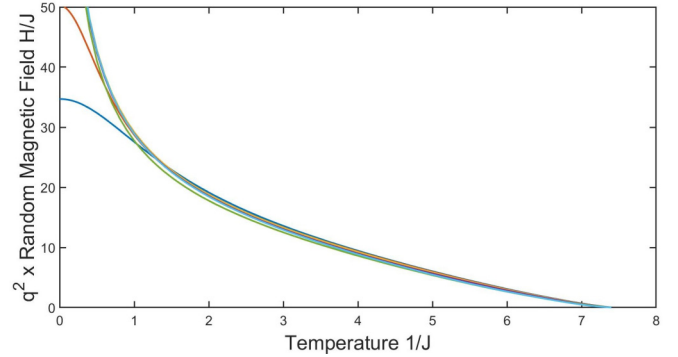


FIG. 3. Phase diagrams for $(q = 7, 10, 20, 50, 100, 150)$ -state random-field clock models in $d = 3$. At low temperature, the curves are, from low field to high field, $q = 7, 10$ and indistinguishably $q = 20, 50, 100, 150$. It is seen that when the random field is scaled with q^2 , a universal phase diagram is found above low temperature for high q .

renormalized nearest-neighbor Hamiltonian. This is repeated 5000 times and the renormalized distribution is obtained. Each nearest-neighbor Hamiltonian in the distribution is exponentiated and thus kept as a transfer matrix [24,38]. To conserve, in this distribution, the $(ij) \leftrightarrow (ji)$ and the random-field direction symmetries, each transfer matrix is replicated by its transpose and by the simultaneous cyclic permutations of the rows and columns. Of the resulting $2q \times 5000$ matrices, 5000 are randomly chosen. Thus, the distribution continues as 5000 $q \times q$ matrices. We have ascertained that our results do not vary with increasing the number 5000 of realizations.

The flows of the distributions determine the phase diagram: Renormalization-group trajectories starting in the ferromagnetic phase flow to the strong-coupling sink of $J_{ij} \rightarrow \infty, H_i = 0$. Renormalization-group trajectories starting in the disordered phase flow to the decoupled sink of $J_{ij}, H_i = 0$. The boundaries between these flow basins are the phase boundaries.

III. $d = 3$ DIMENSIONS AND ZERO-TEMPERATURE CRITICALITY SEGMENT

Our calculated phase diagrams for $(q = 7, 10, 20, 50, 100, 150)$ -state random-field clock models in $d = 3$ are in

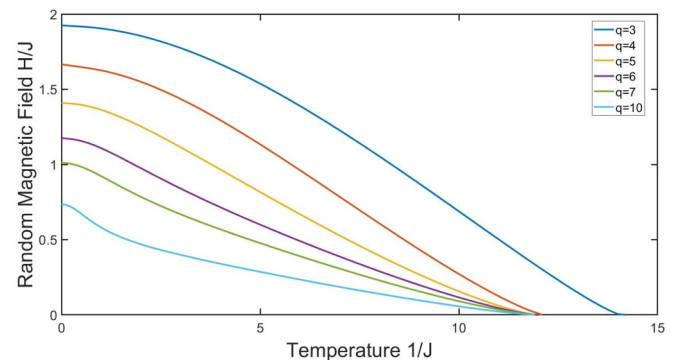


FIG. 4. Phase diagrams for $(q = 3, 4, 5, 6, 7, 10)$ -state random-field clock models in $d = 3.32$, occurring in the figure, respectively, from high field to low field.

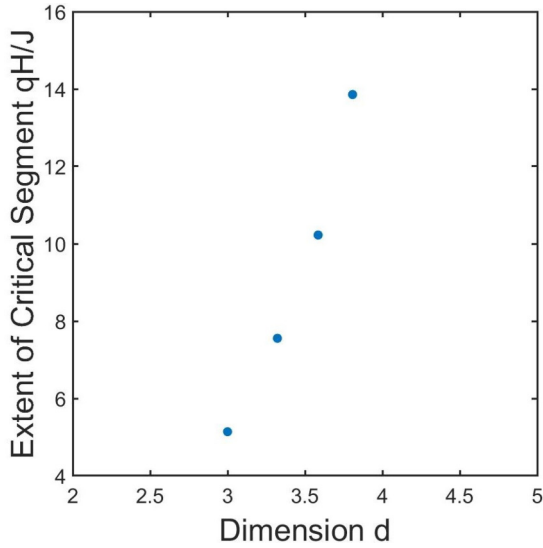


FIG. 5. The critical line segment, at zero temperature, is between $qH/J = 0$ and the qH/J values shown in this figure for each dimension d . The values are consistent with a divergence as $d = 4$ is approached.

Fig. 2, occurring in the figure respectively from high field to low field. Disordered and ferromagnetic phases occur at high temperature, high field and low temperature, low field, respectively. The H/J values on the vertical axis are multiplied with q , originally for better graphical visibility, but eventually leading to a physical result, as seen here. First, note that the ferromagnetic region under random fields recedes and disappears as q is increased. This result is even more evident when we recall that the vertical axis values are amplified by a factor of q for better pictorial visibility. The ferromagnetic phase, in random field, disappearing as $q \rightarrow \infty$, indicates that no ferromagnetic phase occurs in the random-field XY model at nonzero temperature in $d = 3$.

Second, and quite interestingly, given our choice of vertical axis values, it revealed that the ordered phase extends at very low temperatures, for the high q to the universal value of $qH/J = 5.1$. This is more visible in the left inset of Fig. 2. Thus, at $q \rightarrow \infty$, a line segment of zero-temperature critical points occurs between $qH/J = 0$ and $qH/J = 5.1$. Zero-temperature critical segments and multicritical points have been found before, under exact renormalization-group treatment, in the $d = 1$ Blume-Emery-Griffiths model [46].

Third, for high q , the zero-field ferromagnetic transition temperature saturates, as also seen in Ref. [24] and in detail in the right inset in Fig. 2. Furthermore, when the vertical axis is scaled, not by q , but by q^2 , a universal phase diagram emerges above low temperature for high q , as seen in Fig. 3.

IV. $d = 4$ DIMENSIONS AND LOWER CRITICAL DIMENSION

The phase diagrams for $(q = 3, 4, 5, 6, 7, 10)$ -state random-field clock models in $d = 3.32$ are shown in Fig. 4. It is again seen that the ferromagnetic phase, under random fields, recedes and disappears as $q \rightarrow \infty$. Thus, no ferromagnetic phase occurs under random fields in the XY

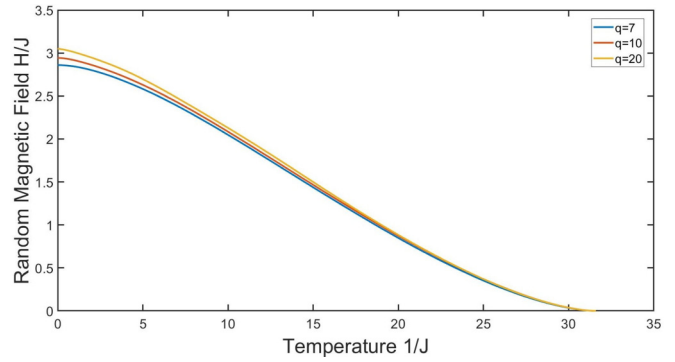


FIG. 6. Phase diagrams for $(q = 7, 10, 20)$ -state random-field clock models in $d = 4$, occurring in the figure, respectively, from low field to high field.

model in $d = 3.32$. However, our calculation again gives the zero-temperature critical segment, between $qH/J = 0$ and $qH/J = 7.6$ universally for all q in $d = 3.32$.

The same results are obtained for $d = 3.58$ and 3.81 , with the zero-temperature critical segment expanding, reaching $qH/J = 10.2$ and 13.9 , respectively. (The volume rescaling factor of a hierarchical lattice, b^d , is equal to the number of bonds being replaced by one bond in the transformation. The length rescaling factor b is equal to the number of bonds on the path between the external spins of the graph. Thus, only discrete values of the dimension d are realized [32].)

A qualitatively different picture occurs in the phase diagrams for $d = 4$, seen in Figs. 5 and 6. Going from $q = 7$ to $q = 10$, the ferromagnetic phase slightly expands in the random field, as opposed to drastically receding as in the lower dimensions. Going from $q = 10$ to $q = 20$, a much larger q interval, the ferromagnetic phase even more slightly expands in the random field. Thus, the ferromagnetic phase occurs, under random fields, for $q \rightarrow \infty$ and for the XY model in $d = 4$. We thus see that the lower critical dimension for the random-field XY model is between $d = 3.81$ and $d = 4$, namely $3.81 < d_c < 4$.

V. CONCLUSION

In order to investigate the random-field XY model, we have studied the random-field q -state clock models for increasing q , for dimensions $d = 3, 3.32, 3.58, 3.81, 4$. We find that for the random-field XY model, the lower critical dimension is between $d = 3.81$ and $d = 4$, namely $3.81 < d_c < 4$. At $d < d_c$, we find a zero-temperature segment of criticality, stretching from zero to a value of qH/J that is q independent for large q and that increases as d_c is approached.

Our calculation is exact for hierarchical lattices. For hypercubic lattices, the Migdal-Kadanoff approximation is an approximation, be it physically intuitive. However, it has done very well with respect to lower critical dimension results for other systems, be it nonrandom or quenched random, as listed in Sec. I.

ACKNOWLEDGMENTS

Support by the Academy of Sciences of Turkey (TÜBA) is gratefully acknowledged.

- [1] D. P. Belanger, A. R. King, and V. Jaccarino, Random-Field Effects on Critical Behavior of Diluted Ising Antiferromagnets, *Phys. Rev. Lett.* **48**, 1050 (1982).
- [2] P.-Z. Wong and J. W. Cable, Hysteretic behavior of the diluted random-field Ising system $Fe_{0.70}Mg_{0.30}Cl_2$, *Phys. Rev. B* **28**, 5361 (1983).
- [3] A. N. Berker, Ordering under random fields: Renormalization-group arguments, *Phys. Rev. B* **29**, 5243 (1984).
- [4] H. Yoshizawa, R. A. Cowley, G. Shirane, R. J. Birgeneau, H. J. Guggenheim, and H. Ikeda, Random-Field Effects in Two- and Three-Dimensional Ising Antiferromagnets, *Phys. Rev. Lett.* **48**, 438 (1982).
- [5] M. S. Cao and J. Machta, Migdal-Kadanoff study of the random-field Ising model, *Phys. Rev. B* **48**, 3177 (1993).
- [6] A. Falicov, A. N. Berker, and S. R. McKay, Renormalization-group theory of the random-field Ising model in 3 dimensions, *Phys. Rev. B* **51**, 8266 (1995).
- [7] A. Aharony, Y. Imry, and S.-K. Ma, Lowering of Dimensionality in Phase Transitions with Random Fields, *Phys. Rev. Lett.* **37**, 1364 (1976).
- [8] A. A. Migdal, Phase transitions in gauge and spin lattice systems, *Zh. Eksp. Teor. Fiz.* **69**, 1457 (1975) [*Sov. Phys. JETP* **42**, 743 (1976)].
- [9] L. P. Kadanoff, Notes on Migdal's recursion formulas, *Ann. Phys. (NY)* **100**, 359 (1976).
- [10] A. N. Berker and S. Ostlund, Renormalisation-group calculations of finite systems: Order parameter and specific heat for epitaxial ordering, *J. Phys. C* **12**, 4961 (1979).
- [11] R. B. Griffiths and M. Kaufman, Spin systems on hierarchical lattices: Introduction and thermodynamic Limit, *Phys. Rev. B* **26**, 5022R (1982).
- [12] M. Kaufman and R. B. Griffiths, Spin systems on hierarchical lattices: 2. Some examples of soluble models, *Phys. Rev. B* **30**, 244 (1984).
- [13] C. T. G. dos Santos, A. P. Vieira, S. R. Salinas, and R. F. S. Andrade, Real-space renormalization-group treatment of the Maier-Saupe-Zwanzig model for biaxial nematic structures, *Phys. Rev. E* **103**, 032111 (2021).
- [14] K. Jiang, J. Qiao, and Y. Lan, Chaotic renormalization flow in the Potts model induced by long-range competition, *Phys. Rev. E* **103**, 062117 (2021).
- [15] G. Mograby, M. Derevyagin, G. V. Dunne, and A. Teplyaev, Spectra of perfect state transfer Hamiltonians on fractal-like graphs, *J. Phys. A: Math. Theor.* **54**, 125301 (2021).
- [16] I. Chio and R. K. W. Roeder, Chromatic zeros on hierarchical lattices and equidistribution on parameter space, *Ann. Inst. Henri Poincaré D*, **8**, 491 (2021).
- [17] B. Steinhurst and A. Teplyaev, Spectral analysis on Barlow and Evans' projective limit fractals, *J. Spectr. Theory* **11**, 91 (2021).
- [18] A. V. Myshlyavtsev, M. D. Myshlyavtseva, and S. S. Akimenko, Classical lattice models with single-node interactions on hierarchical lattices: The two-layer Ising model, *Physica A* **558**, 124919 (2020).
- [19] M. Derevyagin, G. V. Dunne, G. Mograby, and A. Teplyaev, Perfect quantum state transfer on diamond fractal graphs, *Quant. Info. Proc.* **19**, 328 (2020).
- [20] S.-C. Chang, R. K. W. Roeder, and R. Shrock, q-Plane zeros of the Potts partition function on diamond hierarchical graphs, *J. Math. Phys.* **61**, 073301 (2020).
- [21] C. Monthus, Real-space renormalization for disordered systems at the level of large deviations, *J. Stat. Mech.: Theory Exp.* (2020) 013301.
- [22] O. S. Sariyer, Two-dimensional quantum-spin-1/2 XXZ magnet in zero magnetic field: Global thermodynamics from renormalisation group theory, *Philos. Mag.* **99**, 1787 (2019).
- [23] A. Khatun and S. M. Bhattacharjee, Boundaries and Unphysical Fixed Points in Dynamical Quantum Phase Transitions, *Phys. Rev. Lett.* **123**, 160603 (2019).
- [24] E. C. Artun and A. N. Berker, Complete density calculations of q-state Potts and clock models: Reentrance of interface densities under symmetry breaking, *Phys. Rev. E* **102**, 062135 (2020).
- [25] J. V. José, L. P. Kadanoff, S. Kirkpatrick, and D. R. Nelson, Renormalization, vortices, and symmetry-breaking perturbations in 2-dimensional planar model, *Phys. Rev. B* **16**, 1217 (1977).
- [26] A. N. Berker and D. R. Nelson, Superfluidity and phase separation in Helium films, *Phys. Rev. B* **19**, 2488 (1979).
- [27] E. Tunca and A. N. Berker, [arXiv:2202.06049](https://arxiv.org/abs/2202.06049) [cond-mat.stat-mech].
- [28] S. Franz, G. Parisi, and M. A. Virasoro, Interfaces and lower critical dimension in a spin-glass model, *J. Phys. I France* **4**, 1657 (1994).
- [29] C. Amoruso, E. Marinari, O. C. Martin, and A. Pagnani, Scalings of Domain Wall Energies in Two Dimensional Ising Spin Glasses, *Phys. Rev. Lett.* **91**, 087201 (2003).
- [30] J.-P. Bouchaud, F. Krzakala, and O. C. Martin, Energy exponents and corrections to scaling in Ising spin glasses, *Phys. Rev. B* **68**, 224404 (2003).
- [31] S. Boettcher, Stiffness of the Edwards-Anderson Model in all Dimensions, *Phys. Rev. Lett.* **95**, 197205 (2005).
- [32] M. Demirtaş, A. Tuncer, and A. N. Berker, Lower-critical spin-glass dimension from 23 sequenced hierarchical models, *Phys. Rev. E* **92**, 022136 (2015).
- [33] A. Maiorano and G. Parisi, Support for the value 5/2 for the spin glass lower critical dimension at zero magnetic field, *Proc. Natl. Acad. Sci. USA* **115**, 5129 (2018).
- [34] B. Atalay and A. N. Berker, A lower lower-critical spin-glass dimension from quenched mixed-spatial-dimensional spin glasses, *Phys. Rev. E* **98**, 042125 (2018).
- [35] S. R. McKay, A. N. Berker, and S. Kirkpatrick, Spin-Glass Behavior in Frustrated Ising Models with Chaotic Renormalization-Group Trajectories, *Phys. Rev. Lett.* **48**, 767 (1982).
- [36] S. R. McKay, A. N. Berker, and S. Kirkpatrick, Amorphously packed, frustrated hierarchical models: Chaotic rescaling and spin-glass behavior, *J. Appl. Phys.* **53**, 7974 (1982).
- [37] A. N. Berker and S. R. McKay, Hierarchical models and chaotic spin glasses, *J. Stat. Phys.* **36**, 787 (1984).
- [38] S. E. Gürlleyen and A. N. Berker, Asymmetric phase diagrams, algebraically ordered BKT phase, and peninsular Potts flow structure in long-range spin glasses, *Phys. Rev. E* **105**, 024122 (2022).
- [39] T. Çağlar and A. N. Berker, Chiral Potts spin glass in $d = 2$ and 3 dimensions, *Phys. Rev. E* **94**, 032121 (2016).
- [40] H. Y. Devre and A. N. Berker, First-order to second-order phase transition changeover and latent heats of q-state Potts models in $d=2, 3$ from a simple Migdal-Kadanoff adaptation, *Phys. Rev. E* **105**, 054124 (2022).

- [41] D. F. de Albuquerque, S. R. L. Alves, A. S. de Arruda, and N. O. Moreno, Critical behavior in a random field classical XY model for amorphous systems, *Phys. B: Condens. Matter* **384**, 212 (2006).
- [42] T. Kawaguchi, Plastic flow in a driven random-field XY model, *Phys. Lett. A* **251**, 73 (1999).
- [43] K. Okamoto, Alternating $s=1/2$ XY chain in the Lorentzian random field, *J. Phys. Soc. Jpn.* **59**, 4286 (1990).
- [44] H. Nishimori, One-dimensional XY model in Lorentzian random field, *Phys. Lett. A* **100**, 239 (1984).
- [45] L. A. Turkevich, Quantum 1D XY model with random fields, *Bul. Am. Phys. Soc.* **25**, 278 (1980).
- [46] S. Krinsky and D. Furman, Exact renormalization group exhibiting tricritical fixed point for a spin-one Ising model in one dimension, *Phys. Rev. B* **11**, 2602 (1975).